Dramatic Influence of Curing Temperature on Micro–Nano Structure Transform of HNBR Filled with Zinc Dimethacrylate

Zheng Wei,[1] Yonglai Lu,[1,2] Shouke Yan,[1] Yang Meng,[1] Liqun Zhang[1,2]

[1]*Key Laboratory of Beijing City for Preparation and Processing of Novel Polymer Materials, Beijing University of Chemical Technology, Beijing 100029, China*
[2]*Key Laboratory for Nanomaterials of Ministry of Education, Beijing University of Chemical Technology, Beijing 100029, China*

Received 18 January 2011; accepted 31 March 2011
DOI 10.1002/app.34615
Published online 4 October 2011 in Wiley Online Library (wileyonlinelibrary.com).

ABSTRACT: The influence of the curing temperature on micro-nano structure transform of hydrogenated nitrile-butadiene rubber (HNBR) reinforced by zinc dimethacrylate (ZDMA) through *in situ* polymerization was studied by means of Scanning electron microscopy, transmission electron microscopy, Fourier transform infrared spectroscopy, and X-ray diffraction. The results showed that both the amount and diameter of the poly-ZDMA aggregates increased and the graft ratio of poly-ZDMA decreased with the increase of curing temperature. Meanwhile, with the increase of curing temperature, the maximum torque of the curing curve, the crosslinking density (especially for the ionic crosslinking density), and the mechanical properties of HNBR/ZDMA composite decreased significantly. We put forward a possible mechanism that can well explain the phenomenon observed in this work. © 2011 Wiley Periodicals, Inc. J Appl Polym Sci 124: 288–295, 2012

Key words: zinc dimethacrylate; HNBR; crosslinking; nanocomposites; reinforcement

INTRODUCTION

Reinforcement of elastomers is as important as the toughening of plastics. It was well known that nano-sized fillers, such as carbon black, fumed or precipitated silica, and nanodispersed clay, could greatly reinforce elastomers. In recent years, the addition of metal salts of unsaturated carboxylic acids as reactive fillers to elastomers has become a new approach to achieve sustainable reinforcement,[1–3] although the reinforcing effect depends on the type of both the matrix elastomer and the salt.[4–29]

The dramatic reinforcement of hydrogenated nitrile-butadiene rubber (HNBR) by zinc dimethacrylate (ZDMA) was first discovered in the late 1980s. Now, because of the excellent overall properties of HNBR/ZDMA composite, some industrial productions of this composite have been developed, such as the manufacture of tank track rubber pad with excellent strength and abrasion resistance, a component used in oil fields and automobiles.[3,4,23–25]

Nomura et al.[27] first investigated the course of nanodispersed ionic cluster structure of poly-ZDMA in HNBR matrix during peroxide curing, and brought out the point that *in situ* polymerization of ZDMA generated an ionic cluster structure. According to previous researches, there are many factors that can dramatically affect the micro–nano structure transform and properties of elastomers reinforced by ZDMA. Klingender et al.[4] found that high polarity of matrix, suitable reactivity of reaction between rubber and free radicals, and tensile-induced crystallization of rubber might be important factors to enhance the reinforcing effect of ZDMA. Saito et al.[26] investigated the polymerization behavior of ZDMA in HNBR and found that the conversion of ZDMA increased with the peroxide concentration but could hardly exceed 90%. Ikeda et al.[6–8] revealed that the molecular weight and graft ratio of poly-ZDMA depended on the double bond content of the HNBR. Lu et al.[19,28,29] suggested that the dimensions of the ionic cluster increased with ZDMA loading but decreased with increasing peroxide loading. For highly saturated elastomer matrices, most peroxide radicals should attack the ZDMA monomers to initiate the *in situ* polymerization of these monomers at the beginning of curing, and the dimensions of the ionic clusters of poly-ZDMA increased. Several studies[4,14,17,20,23] reported that the ZDMA prepared *in situ* through the

Correspondence to: L. Zhang (zhanglq@mail.buct.edu.cn).
Contract grant sponsor: National Science Fund for Distinguished Young Scholars; contract grant number: 50725310.
Contract grant sponsor: Cheung-kong Scholars Program of the Ministry of Education, China.
Contract grant sponsor: National High Technology Research and Development Program of China; contract grant number: 2009AA03Z338.

neutralization reaction between ZnO and methyl acrylic acid under mixing can achieve a higher conversion than that added directly, and the elastomers reinforced by the ZDMA prepared in this way showed better mechanical properties.

It is well known that curing temperature is a very important factor for elastomer processing to obtain the best properties and production efficiency. In this article, we report for the first time that there were dramatic influences of curing temperature on the micro–nano structure transform and properties (including morphology, vulcanization behavior, crosslink structure, and mechanical properties) of HNBR/ZDMA composite. Furthermore, we put forward a possible mechanism that can well explain the phenomenon observed in this work.

EXPERIMENTAL

Raw materials and formulation

The matrix rubber used in this study was HNBR (Zetpol 2010L, bound nitrile 36%, produced by Zeon Co., Ltd., Tokyo, Japan). ZDMA was supplied by Sartomer Co., Ltd., Exton, Pennsylvania, USA. The dicumyl peroxide (DCP) (AkzoNoble Chemicals Co., Ltd., Nanjing, China) and triallyl isocyanurate (TAIC) (WahSing Chemical Co., Ltd., Jiangsu, China) were commercial products. The formulation of the HNBR/ZDMA compound contained 100 phr HNBR, 30 phr ZDMA, 4 phr DCP, and 1 phr TAIC.

Preparation of specimens

The compound described above was mixed on a 6-inch two-roll mill and compression molded in a hot press for the optimum curing time T_{90} as determined by a rotorless curemeter at a given curing temperatures (140–180°C in 10°C intervals).

Fourier transform infrared spectroscopy

The Fourier transform infrared spectroscopy (FTIR) analyses were performed on an FTIR spectrometer (Tensor 27 from Bruker Optik, Gemany). The scan range was 7800 to 370 cm^{-1} with a resolution of 0.5 cm^{-1}.

X-ray diffraction

The X-ray diffraction (XRD) analyses were carried out on a Rigaku D/Max 2500VBZt/PC X-ray diffractometer (Rigaku, Sendagaya, Japan) with an incident X-ray with a wavelength of about 1.54 Å (Cu Kα radiation at 40 kV and 200 mA). The range of scattering angle (2θ) was 3 to 90°.

Mechanical properties

Tensile tests were performed on a CTM 4104 tensile tester (SANS, Shenzhen, China) at a cross-head speed of 500 mm/min and a temperature of 23 ± 2°C according to Chinese Standards GB/T528-1998 and GB/T529-1999. The shear modulus (G') of HNBR/ZDMA composites cured at different temperatures was investigated by RPA 2000 form Monsanto Company at 60°C, and test frequency is 1 Hz. Flexomete tests were performed on a flexometer at 55°C after 25 min (pressure 1 MPa, stroke 2 mm).

Scanning electron microscopy and transmission electron microscopy

The Scanning electron microscopy (SEM) observations were carried out on an S4700 field emission SEM (Hitachi, Japan). The cured samples were fractured under cryogenic condition with liquid nitrogen, and the compound sheets were cut by a sharp blade to prevent the ZDMA particles from debonding and falling off from the matrix when the samples were fractured. The transmission electron microscopy (TEM) observations were carried out on an H-800 transmission electron microscope (Hitachi, Japan), and the thin sections for TEM experiments were cut by a microtome at −100°C and collected on copper grids.

Measurements of crosslinking density

The crosslinking density was determined by equilibrium swelling. The cured test pieces of HNBR/ZDMA composites were preweighed, placed in a Soxhlet extractor containing butanone, and allowed to swell for 72 h. After extraction, the weights of the swollen wet samples were recorded after the excessive solvent was removed, and then the samples were dried in an oven at 65°C for 24 h and then allowed to stay at room temperature for another 24 h before the weights were recorded again. The total crosslinking density (V_e) was determined according to the Flory-Rehner equation:

$$V_e = -\frac{\ln(1 - V_r) + V_r + \chi V_r^2}{V_1(V_r^{1/3} - V_r/2)} \quad (1)$$

where V_1 is the molar volume of the solvent, χ is the interaction parameter between the solvent and the rubber (the value of $\chi = 0.34$,[21] was used in this work), and V_r is the volume fraction of the composite in the swollen network in equilibrium with the pure solvent.

To distinguish the ionic network from covalent network, samples were swollen in a mixture of toluene and concentrated hydrochloric acid for 5 days to destroy the ionic network, then placed in a Soxhlet extractor containing acetone for 3 days, and vacuum dried. V_{r1}, the covalent crosslinking density, was calculated by using the same formula as eq. (1). V_{r2},

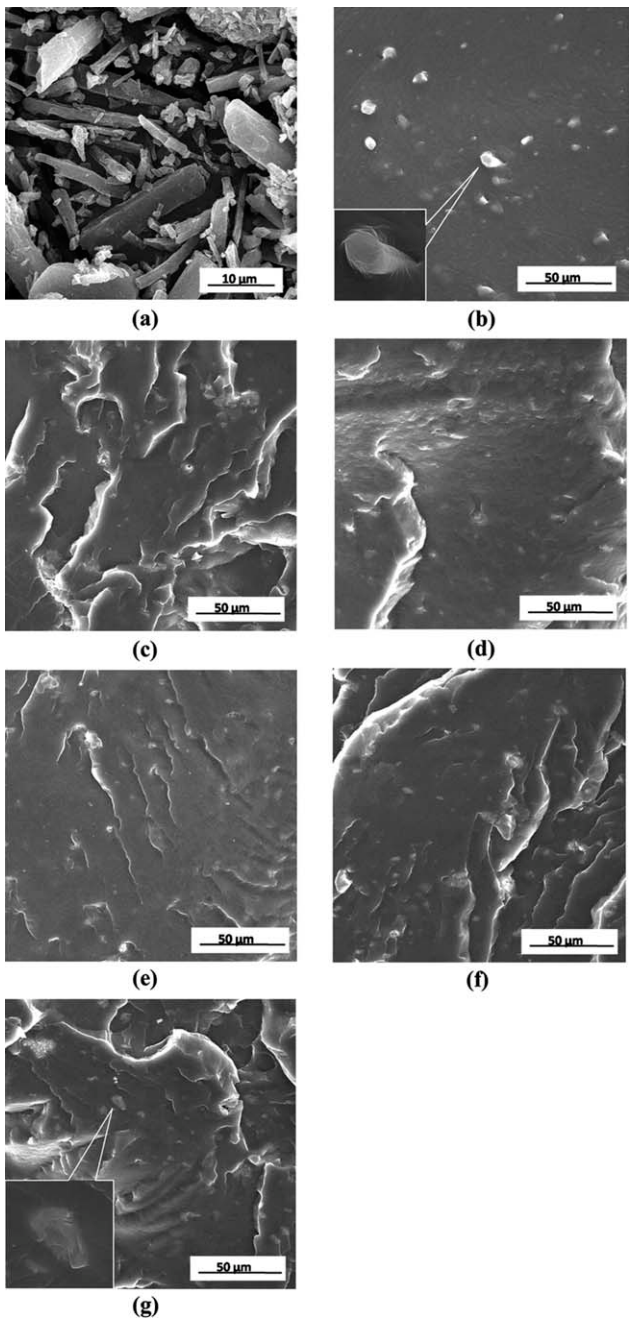

Figure 1 SEM micrographs of (a) ZDMA; (b) HNBR/ZDMA (100/30) compound; and HNBR/ZDMA (100/30) composites cured at different temperatures: (c) 140°C, (d) 150°C, (e) 160°C, (f) 170°C, and (g) 180°C.

the ionic crosslinking density, was calculated by subtracting V_{r1} from V_e.

RESULTS AND DISCUSSION

Morphology analyses

The SEM micrograph of ZDMA powder is shown in Figure 1(a), and that of ZDMA particles dispersed in the HNBR matrix before curing is shown in Figure 1(b). Figure 1(c–g) display the SEM micrographs of various HNBR/ZDMA composites cured at different temperatures. These micrographs clearly indicate that significant amounts of micron-sized particles were present in all cured composites, and both the quantity and the diameter of these particles increased with curing temperature. Furthermore, all observed micron-sized particles on the fracture surface were covered with the matrix, an indication of excellent bonding between these particles and the HNBR matrix after curing process. We can infer from this result that the micron-sized particles are poly-ZDMA aggregates that cannot effectively diffuse into the HNBR matrix during the peroxide curing.

The morphology of HNBR/ZDMA composites on the nanoscale and the ionic clusters obtained by the *in situ* polymerization of ZDMA were observed by means of TEM, as shown in Figure 2. Each of these micrographs demonstrates a large amount of small domains (10–30 nm) that were the poly-ZDMA ionic

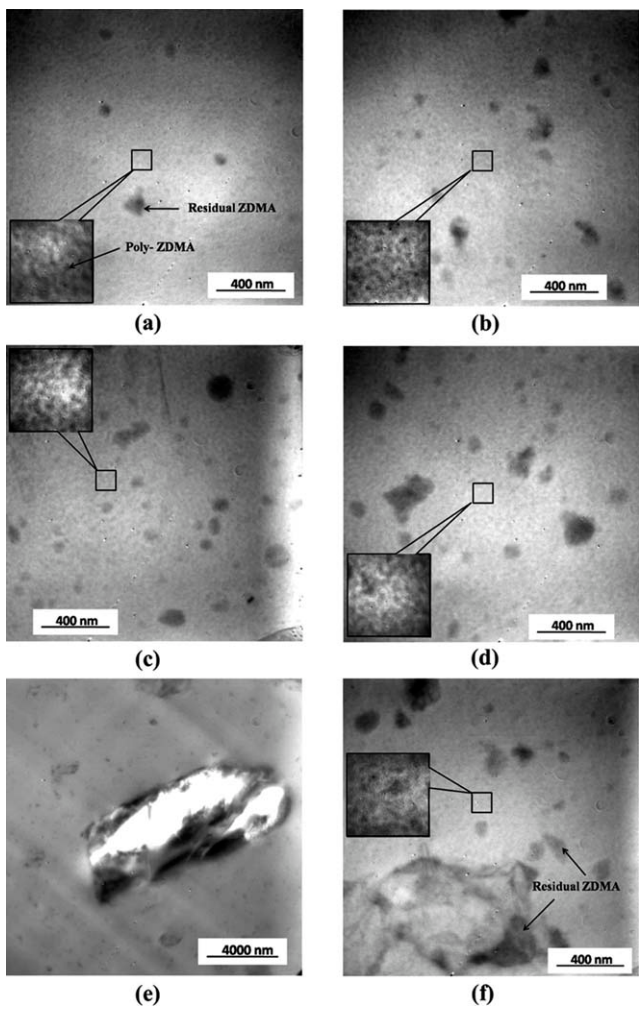

Figure 2 TEM micrographs of HNBR/ZDMA composites cured at different temperatures: (a) 140°C, (b) 150°C, (c) 160°C, (d) 170°C, and (e) and (f) 180°C.

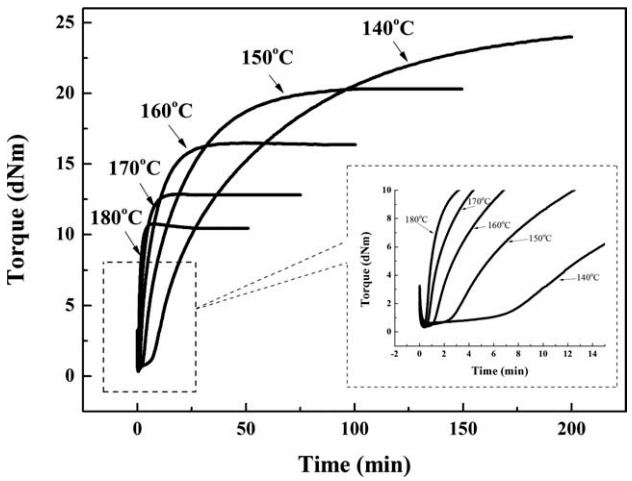

Figure 3 Curing curves of HNBR/ZDMA composites cured at different temperatures.

clusters,[3,26,27,29] along with the larger rounded domains that were the poly-ZDMA aggregates. On the other hand, with the increase of the curing temperature, both the quantity and the diameter of the poly-ZDMA aggregates increased, while the amount of poly-ZDMA ionic clusters decreased (as shown by the amplified insets). Figure 2(f) displays the low-magnification TEM micrograph of the HNBR/ZDMA composite cured at 180°C. The lighter phase was the hole caused by the debonding of micron-sized poly-ZDMA aggregates from the section, and the diameter of the hole was about the same as that of the micron-sized particles observed in the SEM micrograph shown in Figure 1(g).

Vulcanization property

The curing curves of the HNBR/ZDMA compounds cured at different temperatures are shown in Figure 3. It can be clearly observed that there was a noticeable decrease in the maximum torque of HNBR/ZDMA with increasing curing temperature. For a given formulation of HNBR/ZDMA, the higher the crosslinking density, the higher the maximum torque. Therefore, it was reasonable to infer that the decrease of the maximum torque of HNBR/ZDMA with the increase of curing temperature was due to the decrease of the crosslinking density of HNBR/ZDMA.

Crosslinking density

The influence of curing temperature on the crosslink density (including the ionic and the covalent crosslink density) of HNBR/ZDMA composite is shown in Figure 4. With the increase of the curing temperature, both the ionic and the covalent crosslinking density of HNBR/ZDMA decreased sharply (especially in the temperature range 150–160°C). Moreover, the majority (over 85%) of the total crosslink structure was made up of ionic bonds at any curing temperature. It can be concluded that the decrease of total crosslinking density was mainly attributed to the decrease of ionic crosslinking density with the increase of the curing temperature.

Conversion and graft ratio of *in situ* polymerization of ZDMA

There was dramatic influence of the conversion ratio of *in situ* polymerization of ZDMA on the crosslink structures of the elastomer/ZDMA composites because only the poly-ZDMA can actually generate the ionic clusters. The conversion ratio of *in situ* polymerization of ZDMA in the HNBR matrix was studied by FTIR analysis, and the results are shown in Figure 5. The band at 1651 cm^{-1} was attributed to the vibration of C=C, and the bands at both 945 and 831 cm^{-1} were attributed to the vibration of C—H on the C=C.[20] After normalization to the —CN (2236 cm^{-1}), which is stable during peroxide curing, all the three bands can be used for the quantitative analysis of the conversion ratio of ZDMA. As shown in Figure 5, the bands at 1651, 945, and 831 cm^{-1} for the specimens cured at any temperature completely disappeared. Consequently, it can be concluded that the curing temperature had no significant effect on the conversion ratio of *in situ* polymerization of ZDMA in HNBR.

To further verify the conversion ratio of the *in situ* polymerization of ZDMA during the curing process, XRD analysis was used to prove the structural change of ZDMA crystals in both the uncured compound and cured composites, with the expectation that the *in situ* polymerization may result in the conversion of ZDMA from the crystalline to amorphous state.[17,20,21,23] As shown in Figure 6, the ZDMA crystals in the uncured HNBR/ZDMA compound

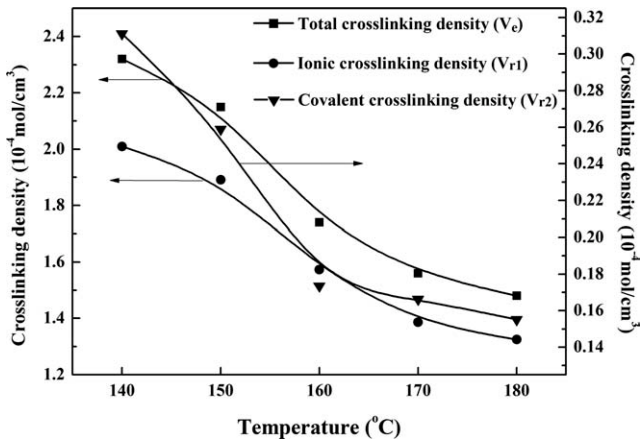

Figure 4 Influence of curing temperature on crosslinking density of HNBR/ZDMA composites.

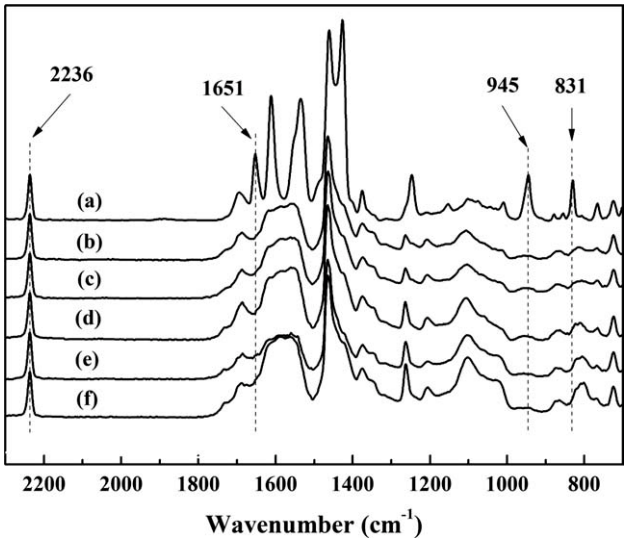

Figure 5 FTIR spectra of HNBR/ZDMA compound and composites cured at different temperatures: (a) uncured HNBR/ZDMA compound; (b)-(f) HNBR/ZDMA composites cured at different temperatures: (b) 140°C, (c) 150°C, (d) 160°C, (e) 170°C, and (f) 180°C.

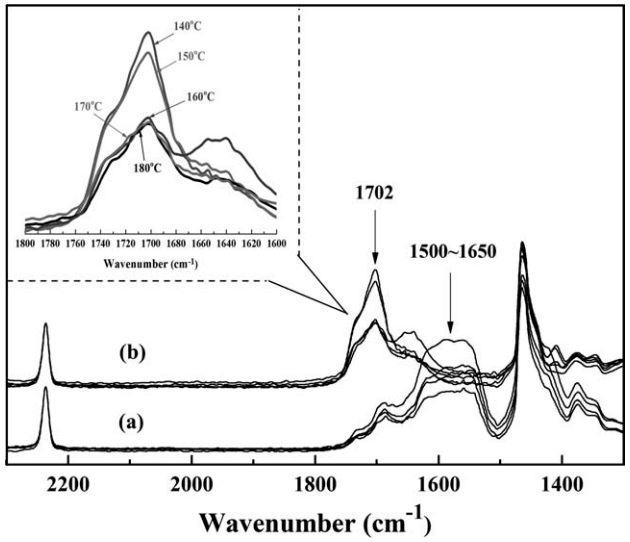

Figure 7 FTIR spectra of HNBR/ZDMA composites: (a) before and (b) after hydrolysis and Soxhlet extraction treatment.

presented several sharp diffraction peaks because of the high crystallinity of these particles. However, it was surprising that all these diffraction peaks completely disappeared after the compound was cured at various temperatures. The results suggest that almost all the ZDMA crystals in the HNBR matrix took part in the *in situ* polymerization during peroxide curing process, so there was no significant change in the conversion ratio of ZDMA with curing temperatures. Therefore, in conjunction with the FTIR and XRD results, the conversion ratio of ZDMA may be not the main reason for the decrease of ionic crosslinking density with increasing curing temperature.

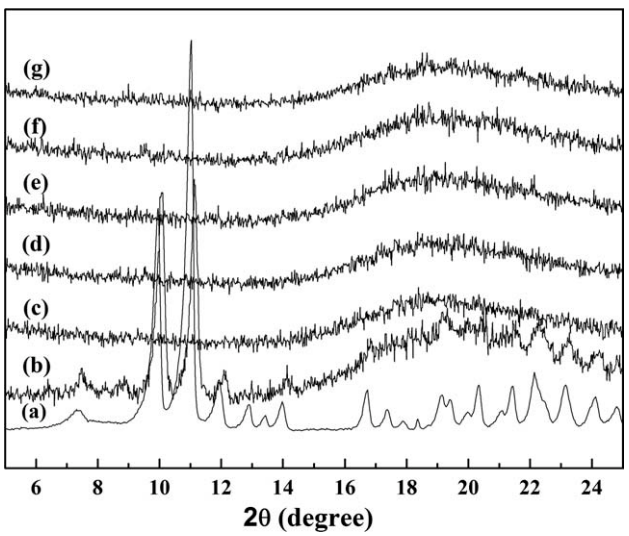

Figure 6 XRD patterns of HNBR/ZDMA composites: (a) pure ZDMA particles; (b) uncured HNBR/ZDMA compound; (c)-(g) HNBR/ZDMA composites cured at different temperatures: (c) 140°C, (d) 150°C, (e) 160°C, (f) 170°C, and (g) 180°C.

The samples of HNBR/ZDMA composites before and after hydrolysis and Soxhlet extraction treatment, which is used to destroy the ionic crosslink structure (see Measurements of Crosslinking Density and Crosslinking Density sections for details), were studied by FTIR. The results given in Figure 7 show that the broad asymmetric bands for —COO— at 1500–1650 cm^{-1} disappeared after the hydrolysis and Soxhlet extraction treatment, while a new stretching vibration band (associated with —COOH) appeared at 1702 cm^{-1}. These results confirmed that the hydrolysis of poly-ZDMA had been quite thorough, and almost all the Zn^{2+} had been replaced by H^+ during hydrolysis. On the other hand, these results also confirmed that parts of the poly-ZDMA were grafted on the HNBR matrix chain during peroxide curing, because any ungrafted poly-ZDMA and residual unreacted ZDMA can be extracted from the samples during the Soxhlet extraction treatment. Moreover, it can be observed from the upper left inset that after normalization with the —CN band for HNBR, the intensity of the bands associated with —COOH was much higher for the samples cured at 140 and 150°C than for the samples cured at 160–180°C. It can be concluded that higher graft ratio between the poly-ZDMA and HNBR can be obtained when the curing temperature was lower than 160°C. Because, only the grafted poly-ZDMA can actually generate the ionic crosslink structure in HNBR/ZDMA composites, with a similar conversion ratio of ZDMA, and it can be reasonably confirmed that the sharp decrease of ionic crosslinking

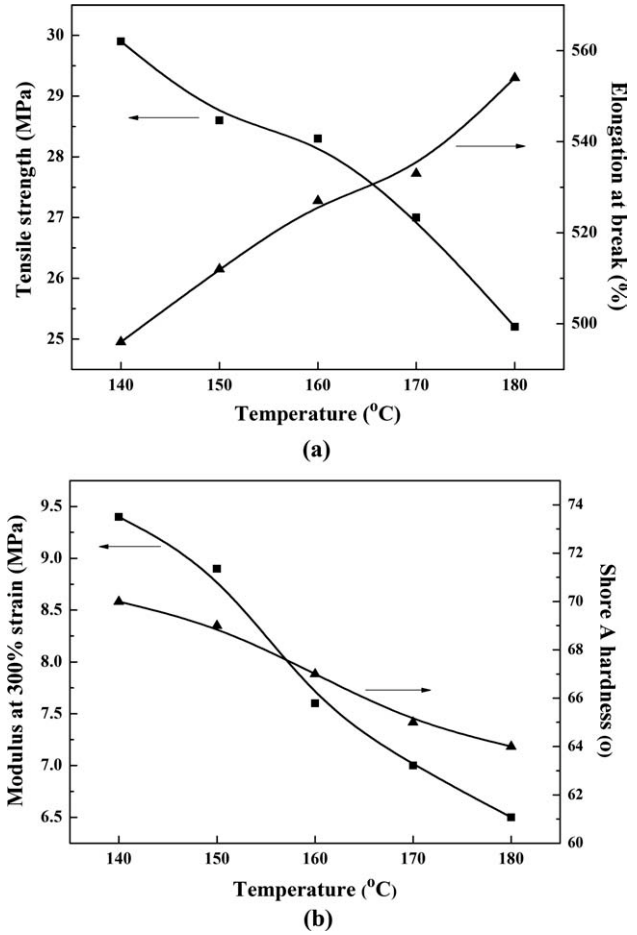

Figure 8 Influence of curing temperature on mechanical properties of HNBR/ZDMA composites: (a) tensile strength and elongation at break; (b) modulus at 300% strain and Shore A hardness

density with increasing curing temperature (especially from 150 to 160°C) was mainly caused by the dramatic decrease of the graft ratio of poly-ZDMA.

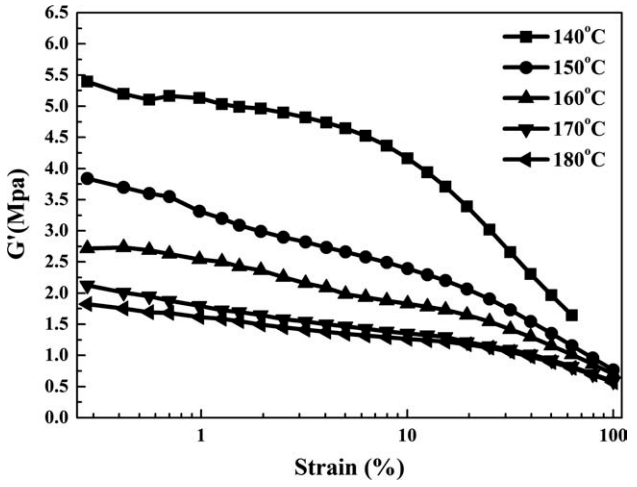

Figure 9 Influence of curing temperature on shear modulus (G′) of HNBR/ZDMA composites

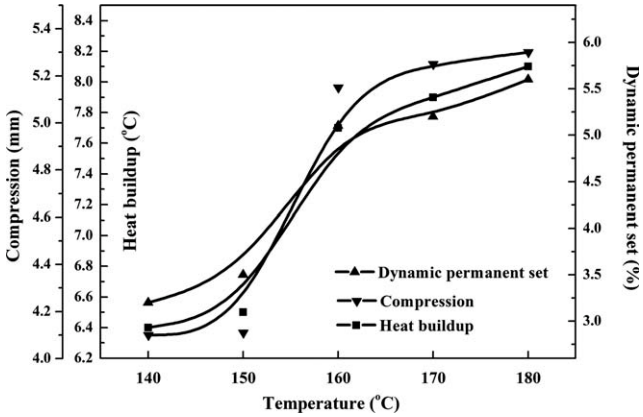

Figure 10 Influence of curing temperature on flexometer heat buildup, dynamic permanent set, and compression of HNBR/ZDMA composites

Mechanical properties

Morphology and structure are important factors governing the properties of HNBR/ZDMA composites. With increasing curing temperature, the poor dispersion of poly-ZDMA and the decrease of the ionic crosslinking density can result in the changes of the mechanical properties of the HNBR/ZDMA composites.

It can be seen from Figure 8 that the tensile strength, modulus at 300% elongation, and Shore A hardness of the HNBR/ZDMA composite dramatically decreased and the elongation at break increased with the increase of the curing temperature. Besides, as shown in Figure 9, the shear modulus (*G*′) of HNBR/ZDMA composites increased with the decrease of curing temperature at any shear strain. Especially, a plateau can be observed at the curing temperature of 140°C, implying the existence of a strong ionic bond crosslink network in HNBR/ZDMA composite. Moreover, the results of flexometer tests revealed that the HNBR/ZDMA composite exhibited a marked increase in heat buildup, dynamic permanent set, and compression with the curing temperature, as shown in Figure 10. In particular, all the three properties showed a dramatic increase when the curing temperature increased from 150 to 160°C.

DISCUSSION

On the basis of previous researches,[19,26–29] it is well accepted that the *in situ* polymerization of ZDMA is mainly determined by the balance of "dissolving diffusion," which causes the ZDMA monomers to continuously diffuse into the HNBR matrix to take part in *in situ* polymerization. The above procedure is repeated continuously during the peroxide curing process. Finally, the majority of the original ZDMA particles dispersed in the rubber matrix disappear,

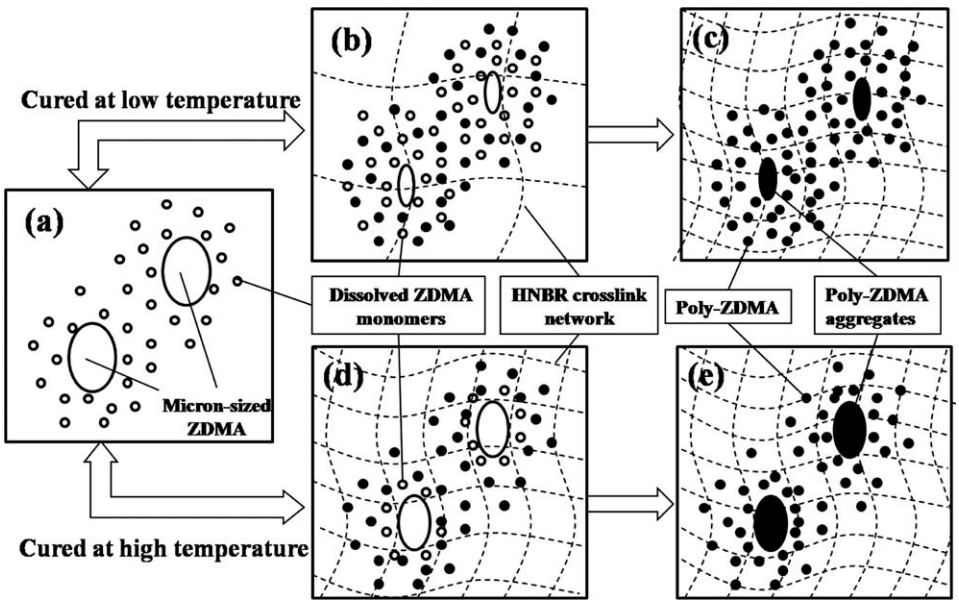

Figure 11 Schematic representation of 'dissolving-diffusion' process of ZDMA in HNBR matrix induced by their *in situ* polymerization during peroxide curing at high and low curing temperatures.

and many nanodispersions of 10–30 nm diameter are formed in the cured HNBR matrix.

In this article, we consider that there was dramatic influence of curing temperature on the "dissolving diffusion" process of ZDMA in the HNBR matrix during peroxide curing, finally resulting in the variation of both the graft ratio and the dispersion level of poly-ZDMA with curing temperature. A schematic representation of the "dissolving diffusion" process of ZDMA particles in the HNBR matrix induced by their *in situ* polymerization during peroxide curing at high and low curing temperatures is shown in Figure 11.

As shown in Figure 11(a), there are both ZDMA monomers that were originally dissolved in the HNBR matrix during the mixing process and micron-sized ZDMA particles in HNBR matrix. At the beginning of curing process, the originally dissolved ZDMA monomers preferentially took part in the *in situ* polymerization; meanwhile, new ZDMA monomers [shown as white dots in Fig. 11(b,d)] continuously dissolved in the HNBR matrix away from ZDMA particles because of the "dissolving diffusion" balance of ZDMA in the matrix. However, there was dramatic influence of curing temperature on this "dissolving diffusion" balance of ZDMA particles, especially for the micron-sized ZDMA particles.

According to the curing curves of HNBR/ZDMA compounds shown in Figure 3, the crosslink network of the HNBR matrix increased much more rapidly at high curing temperatures than at low curing temperatures [depicted in Fig. 11(b,d)]. Under this condition, at high curing temperatures, because of the rapid increase of the viscosity of the HNBR matrix with time, the extent of the "dissolve diffusion" of ZDMA during the curing process is further limited and the *in situ* polymerization of ZDMA becomes diffusion controlled. As shown in Figure 11(c,e), the poor diffused large ZDMA particles can also take part in *in situ* polymerization. However, it was more possible for poorly diffused ZDMA to self-polymerize and form micron-sized poly-ZDMA aggregates. The diameter of the poly-ZDMA aggregates increased with the increase of curing temperature because of the low "dissolving diffusion" level for large ZDMA particles at high curing temperature. Moreover, because the amount of self-polymerized poly-ZDMA increased with curing temperature, it can be explained the decrease of the graft ratio of poly-ZDMA, as shown in Figure 7.

CONCLUSIONS

With increasing the curing temperature, the maximum torque, the crosslinking density (including the ionic and the covalent bonds), and the mechanical properties of HNBR/ZDMA composite decreased significantly. These decreases were mainly caused by the decrease of the graft ratio of poly-ZDMA and the increase of both the amount and diameter of the poly-ZDMA aggregates with the increase of the curing temperature. A possible mechanism for the micro–nano structure transform of ZDMA at different curing temperatures was put forward. We suggested that, with increasing curing temperature, the extent of the "dissolving diffusion" of ZDMA in the HNBR matrix was dramatically limited by the rapid increase of the viscosity of HNBR matrix with time,

finally resulting in the variation of the graft ratio and both the amount and diameter of poly-ZDMA aggregates with curing temperature.

References

1. Hamed, G. R. Rubber Chem Technol 2000, 73, 524.
2. Hamed, G. R. Rubber Chem Technol 2007, 80, 533.
3. Inoue, T. Prog Polym Sci 1995, 20, 119.
4. Klingender, R. C.; Oyama, M.; Satio, Y. Rubber World 1990, 202, 26.
5. Yuan, X. H.; Peng, Z. L.; Zhang, Y.; Zhang, X. F.; Zhang, Y. X. China Synth Rubber Ind 2003, 23, 173.
6. Ikeda, T.; Yamada, B. Polym Int 1999, 48, 367.
7. Ikeda, T.; Yamada, B.; Tsuji, M.; Sakurai, S. Polym Int 1999, 48, 446.
8. Ikeda, T.; Sakurai, S.; Nakano, K.; Yamada, B. J Appl Polym Sci 1996, 59, 781.
9. Zhao, Y.; Lu, Y. L.; Liu, L.; Feng, Y. X.; Zhang, L. Q. China Rubber Synth Ind 2001, 24, 350.
10. Zhao, Y.; Lu, Y. L.; Liu, L.; Feng, Y. X.; Zhang, L. Q. China Rubber Synth Ind 2002, 25, 35.
11. Wu, S. M.; Lu, Y. L.; Gu, L.; Zhang, L. Q. China Rubber Ind 2002, 49, 709.
12. Yin, D. H.; Zhang, Y.; Peng, Z. L.; Zhang, Y. X. Eur Polym J 2003, 39, 99.
13. Du, A. H.; Peng, Z. L.; Zhang, Y.; Zhang, Y. X. Polym Test 2002, 21, 889.
14. Nie, Y. J.; Huang, G. G.; Qu, L. L.; Zhang, P.; Weng, G. S.; Wu, J. R. J Appl Polym Sci 2010, 115, 99.
15. Gao, G. X.; Zhang, Z. C.; Zheng, Y. S.; Jin, Z. H. J Appl Polym Sci 2009, 113, 3901.
16. Yuan, X. H.; Peng, Z. L.; Zhang, Y.; Zhang, Y. X. Polym Polym Compos 1999, 7, 431.
17. Yuan, X. H.; Peng, Z. L.; Zhang, Y.; Zhang, Y. X. J Appl Polym Sci 2000, 77, 2704.
18. Peng, Z. L.; Zhang, Y.; Liang, X.; Zhang, Y. X. Polym Polym Compos 2001, 9, 275.
19. Lu, Y. L.; Liu, L.; Tian, M.; Geng, H. P.; Zhang, L. Q. Eur Polym J 2005, 41, 589.
20. Wang, Y. H.; Peng, Z. L.; Zhang, Y.; Zhang, Y. X. China Rubber Synth Ind 2005, 28, 205.
21. Huang, A. M.; Wang, X. P.; Jia, D. M. China Acta Polymerica Sinica 2007, 12, 1154.
22. Du, A. H.; Peng, Z. L.; Zhang, Y.; Zhang, Y. X. J Appl Polym Sci 2004, 93, 2379.
23. Peng, Z. L.; Liang, X.; Zhang, Y. X.; Zhang, Y. J Appl Polym Sci 2002, 84, 1339.
24. Tocuchet, P.; Rodriguez, G.; Gatza, P. E.; Butler, D. P.; Crawford, D.; Teets, A. R. U.S. Pat. 4,843,114 (1989).
25. Medalia, A. I.; Alesi, A. L.; Mead, J. L. Rubber Chem Technol 1992, 65, 154.
26. Saito, Y.; Nishimura, K.; Asada, M.; Toyoda, A. J Jpn Rubber Soc 1994, 67, 867.
27. Nomura, A.; Takano, J.; Toyoda, A.; Saito, T. J Jpn Rubber Soc 1993, 66, 830.
28. Lu, Y. L.; Liu, L.; Shen, D. Y.; Yang, C.; Zhang, L. Q. Polym Int 2004, 53, 802.
29. Lu, Y. L.; Liu, L.; Yang, C.; Tian, M.; Zhang, L. Q. Eur Polym J 2005, 41, 577.